This article has been accepted for publication in IEEE Access. This is the author's version which has not been fully edited and content may change prior to final publication. Citation information: DOI 10.1109/ACCESS.2023.3348132

IEEE Access
Multidisciplinary | Rapid Review | Open Access Journal

Date of publication xxxx 00, 0000, date of current version xxxx 00, 0000.

Digital Object Identifier 10.1109/ACCESS.2023.Doi Number

Automatic Determination of Set of Multivariate Basis Polynomials Based on Recursion and Application of LSPCR to High-dimensional Uncertainty Quantification of Multi-conductor Transmission Lines

Weiwei Chen, Yuhang Ji, Ziyang Qi, Liping Yan, Senior Member, IEEE, and Xiang Zhao

All authors are affiliated with the College of Electronics and Information Engineering, Sichuan University, Chengdu 610065, China

Corresponding author: Xiang Zhao (e-mail: zhaoxiang@scu.edu.cn).

ABSTRACT Uncertainty quantification (UQ) in polynomial chaos expansion (PCE) suffers from the curse of dimensionality, which is fundamentally reflected in that the number of the PCE coefficients to be found grows rapidly as the number of random inputs increases, and thus the number of samples required increases dramatically. Regardless of the approach taken to alleviate this disaster, we are usually faced with the technical challenge of automatically and programmatically determining the basis functions during the PCE implementation, which are composed of a large number of multivariate polynomials. To address this problem, this paper proposes an algorithm based on the recursive idea for automatically determining the basis functions, and combines this algorithm with the latest weight-based regression called least squares polynomial chaos regression (LSPCR), proposes the implementation of the LSPCR method in the medium- and high-dimensional cases, and evaluates its performance in the electromagnetic coupling problem of the transmission lines (TLs) in this case. Subsequently, the performance of six algorithms for LSPCR are compared in the medium- and high-dimensional, low-order cases, each algorithm consisting of a sampling strategy selected from asymptotic sampling (AS), standard sampling (SS), and coherence-optimal sampling (COS), paired with a norm problem chosen from either least squares optimization (LSO) or ℓ_1-minimization (ℓ_1-M) problems. Numerical experiments demonstrate the excellence of the proposed algorithm. Furthermore, the results also show that only the algorithms that employ the SS (SSs) and the algorithms based on the COS (COSs) require no more than 1.4% of the total Monte Carlo (MC) computation time when producing similarly accurate results to the MC, regardless of the chosen norm problem.

INDEX TERMS uncertainty quantification (UQ), polynomial chaos expansion (PCE), least squares polynomial chaos regression, high dimensionality, transmission lines (TLs).

I. INTRODUCTION

Polynomial chaos expansion (PCE), a prominent method for uncertainty quantification (UQ) in various engineering fields [1]-[18], gradually shows a significant decrease in its efficiency as the count of random parameters increases, i.e., the curse of dimensionality.

In recent years, many efficient techniques have been proposed to alleviate dimensionality disasters. A tensor recovery approach to improve efficiency was proposed in [19], which exploits the sparsity and low-rank properties of some higher-order tensors to compress the number of samples required. [20] discussed a combination of a hierarchical approach and the Stochastic Galerkin (SG) method, where the hierarchical approach is introduced to merge the underlying geometric and material uncertainty parameters into the uncertainty quantities of the associated per-unit-length parameters to achieve dimensionality reduction. In [21], a combination of a decoupled perturbative technique with the SG method was presented, where the decoupling technique allows a better scaling of the number of the PCE coefficients and thus a reduction of the dimensional catastrophe. A new polymorphic formulation based on the generalized PC method was developed in [22], where polymorphic variables can lead to a compression of the dimensionality of random inputs by capturing the combined effect of epistemic and aleatory uncertainties in the system. [23] proposed an algorithm combining partial least squares techniques and the generalized PC method, where a nonlinear partial least squares technique is used to convert a group of random variables (RVs) into a smaller number of uncorrelated ones, followed by dimensionality reduction.

All of these approaches focus on two main ways. One approach is to compress the number of samples required

This work is licensed under a Creative Commons Attribution-NonCommercial-NoDerivatives 4.0 License. For more information, see https://creativecommons.org/licenses/by-nc-nd/4

This article has been accepted for publication in IEEE Access. This is the author's version which has not been fully edited and
content may change prior to final publication. Citation information: DOI 10.1109/ACCESS.2023.3348132

through certain techniques. Another approach is to reduce the dimensionality by compressing the number of random input parameters through certain techniques, which may not work in all high-dimensional UQ problems, or even if they do work in some problems, the dimensionality may still remain high after the reduction. Regardless of the approach taken to alleviate this disaster, we are usually faced with the technical challenge of automatically and programmatically determining the basis functions during the PCE implementation, which are composed of a large number of multivariate polynomials. To address this problem, this paper proposes an algorithm based on the recursive idea for automatically determining the basis functions, and combines this algorithm with the latest weight-based regression called least squares polynomial chaos regression (LSPCR) [24]-[26], proposes the implementation of the LSPCR method in the medium- and high-dimensional cases, and evaluates its performance in the electromagnetic coupling problem of the transmission lines (TLs) in this case. The LSPCR method increases efficiency by compressing the number of samples. It differs from the generally known regression approach. In the latter, the required samples are taken across the entire random space corresponding to the random parameters, and the original stochastic problem is addressed by solving the regression problem without weights over the entire random space. The LSPCR method transforms the original stochastic problem from the entire random space into a suitable subset and solves the weighted regression problem on the subset to obtain the PCE coefficients, where different sampling strategies corresponding to different weights are established, thus obtaining high quality samples to improve efficiency. Six algorithms for LSPCR have been designed and implemented, each consisting of a sampling strategy selected from asymptotic sampling (AS), standard sampling (SS), and coherence-optimal sampling (COS), paired with a norm problem chosen from either least squares optimization (LSO) or ℓ_1-minimization (ℓ_1-M) problems, where the AS and the COS are newly developed sampling strategies based on weights. The six algorithms are then compared in the medium- and high-dimensional, low-order cases.

The results of these comparisons will be the most up-to-date. This is because the difference in performance of these six algorithms is related to the dimensionality of the random input parameters and the highest order of the basis function. Moreover, the comparison of the six algorithms in the low-order, medium-dimensional case, the comparison of the LSO-based algorithms in the low-order, high-dimensional case, and the comparison of the ℓ_1-M-based algorithms in the low-order, high-dimensional case are not considered in [24][25], and [26] only considers the six algorithms in the low-order, low-dimensional case for comparison.

The organization of this paper is as follows: Section II presents the LSPCR implementation scheme for medium- and high-dimensional cases. Section III introduces the application of the LSPCR method to medium- and high-dimensional TL problems. Finally, a conclusion is drawn in Section IV.

II. LSPCR IMPLEMENTATION SCHEME FOR MEDIUM AND HIGH DIMENSIONAL CASES

A. Review of the LSPCR method

Consider the stochastic differential equation

$$\mathcal{L}(\zeta, x, t, w) = \mathcal{H}(\zeta, x, t), \qquad x \in D, \tag{1}$$

where $\mathcal{L}$ is a differential operator, $x \in D \subset \mathbb{R}^m, m = 1, 2, 3$, $\zeta = (\zeta_1, \cdots, \zeta_d)$ is a random vector, and its probability density function (pdf) is ρ with the support Γ. If the components of ζ are independent of each other and all in Askey-scheme [27], and equation (1) has a unique solution $w = w(\zeta, x, t)$ whose variance is bounded, then $w(\zeta, x, t)$ can be approximated as

$$w(\zeta, x, t) \approx \sum_{k=1}^{P} c_k(x, t)\Psi_k(\zeta), \tag{2}$$

with

$$\mathrm{E}[\Psi_m(\zeta)\,\Psi_n(\zeta)] = h_m^2 \delta_{mn},$$

where P is the number of the basis functions $\{\Psi_k(\zeta)\}_{k=1}^{P}$, E denotes the expectation operator, $h_m^2 = \int_\Gamma \Psi_m^2 \rho(\zeta) d\zeta$, δ_{mn} is the Kronecker function. If the highest order of basis functions is p, then $P = \binom{p+d}{d}$.

To obtain the coefficients $\boldsymbol{c} := (c_1, \cdots, c_P)^{\mathrm{T}}$ in (2), the LSPCR method is used. Once the PCE coefficients are obtained, the first two moments of $w(\zeta, x, t)$ can be expressed according to the coefficients $\boldsymbol{c}$.

1) PRINCIPLE OF THE LSPCR METHOD

We take N samples $\{\eta^{(i)}\}_{i=1}^{N}$ by some kind of sampling strategies, and the corresponding solutions of (1) are denoted as $\{w(\eta^{(i)})\}_{i=1}^{N}$,where N is the number of independent samples. Two different weight-based norm problems, including the LSO problem [24], i.e.,

$$\underset{\hat{\boldsymbol{c}}}{\operatorname{argmin}} \parallel \boldsymbol{V}\boldsymbol{w} - \boldsymbol{V}\boldsymbol{\Phi}\hat{\boldsymbol{c}} \parallel_2, \tag{3}$$

and the ℓ_1-M problem [25], i.e.,

$$\underset{\boldsymbol{c}}{\operatorname{argmin}} \parallel \hat{\boldsymbol{c}} \parallel_1 \quad \text{subject to } \|\boldsymbol{V}\boldsymbol{w} - \boldsymbol{V}\boldsymbol{\Phi}\hat{\boldsymbol{c}}\|_2 \le \delta \tag{4}$$

are used to obtain the coefficient $\hat{\boldsymbol{c}}$ in (2), where $\boldsymbol{V}(i,i) = \varphi(\eta^{(i)})$, $\boldsymbol{w} := \left(w(\eta^{(1)}), \cdots, w(\eta^{(N)})\right)^{\mathrm{T}}$, $\boldsymbol{\Phi}(i,j) := \Psi_j(\eta^{(i)})$, and δ is a tolerance for solution imprecision, φ is named the weight function.

2) THREE SAMPLING STRATEGIES

Here we introduce the SS, the AS, and the COS. The AS and the COS have recently been developed based on weights and are unique in that they do not sample based on the pdf $\rho(\eta)$ of ζ in (1), but on a newly constructed distribution. Furthermore, they do not sample over the entire random space Γ as usual, but over a subset of it.

(a) Standard sampling

The SS is to draw samples according to the pdf $\rho(\eta)$ of ζ in (1), and its weight function is $\varphi(\eta) = 1$.

This work is licensed under a Creative Commons Attribution-NonCommercial-NoDerivatives 4.0 License. For more information, see https://creativecommons.org/licenses/by-nc-nd/4

This article has been accepted for publication in IEEE Access. This is the author's version which has not been fully edited and
content may change prior to final publication. Citation information: DOI 10.1109/ACCESS.2023.3348132

(b) Asymptotic sampling

If ζ in (1) is a d-dimensional standard normal random vector, then the AS is to take samples from the uniform distribution supported on a d-dimensional sphere whose radius is $r = \sqrt{2} \cdot \sqrt{2p+1}$. Its samples can be generated by the following algorithm. First, draw samples of $Z := (z_1, \cdots, z_d)$, where $z_1, \cdots, z_d$ independently follow normal distributions with zero mean and the same variance. Second, take samples of U, which is uniformly distributed on [0,1]. Third, take samples of $X = \frac{Z}{\|Z\|_2} \cdot r \cdot U^{\frac{1}{d}}$, which is a uniform distribution of radius r on a d-dimensional sphere. In this case, the weight function is $\varphi(\eta) = \exp(-\| \eta \|_2^2/4)$.

(c) Coherence-optimal sampling

The COS uses $f_X(\eta) := a^2 \rho(\eta) B^2(\eta)$ for sampling, and the weight function is $\varphi(\eta) = \frac{1}{B(\eta)}$, where $B(\eta) := \sqrt{\sum_{k=1}^{p} |\Psi_k(\eta)|^2}$. The procedure for sampling from f_X can be seen in algorithm 1 in [26], which requires a candidate distribution. If ζ in (1) is a standard normally distributed random vector, then the candidate is selected as the standard normal distribution when $p \leqslant d$, and the uniform distribution on a d-dimensional sphere is selected when $p > d$.

The three sampling strategies combined with the two norm problems result in six algorithms. For simplicity of expression, we refer to the algorithm using the SS combined with the LSO technique as SS&LSO, and the others are defined similarly. In addition, COS&LSO and COS& ℓ_1-M are collectively referred to as COSs, while ASs and SSs are similarly named.

B. Automatic determination of the set of basis functions based on recursive ideas

Consider the set consisting of all p-order basis polynomials with d elements, denoted by A. Each element of the set can be expressed as

$$F_p(x_1, x_2, \cdots, x_d) = f_1(x_1) \cdot f_2(x_2) \cdot \cdots \cdot f_d(x_d)$$

with

$$O(f_1(x_1)) + O(f_2(x_2)) + \cdots + O(f_d(x_d)) \leq p,$$

where $O(f_i(x_i))$ $(i = 1, \cdots, d)$ denotes the order of the monic polynomial $f_i(x_i)$ with respect to the ith element x_i.

We already know that the cardinal number of A is

$$\bar{\bar{A}} = \frac{(d+p)!}{d!\,p!}.$$

It can be seen that as d and p increase, $\bar{\bar{A}}$ also increases rapidly. For example, $d = 26$, $p = 4$ results in $\bar{\bar{A}} = 27405$. Therefore, to implement the LSPCR method in the high-dimensional, high-order case, it is necessary to design an algorithm that can be universally applied to automatically generate all the elements of A when d and p take arbitrary values.

Denote $p_i = O(f_i(x_i))$, then we have

$$p_1 + p_2 + \cdots + p_d \leq p,$$

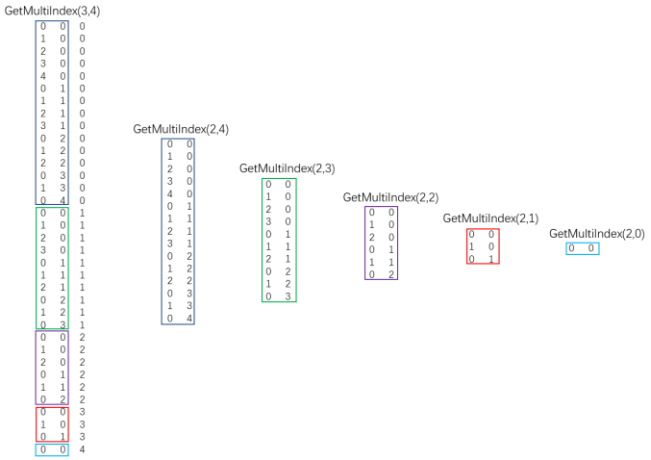

FIGURE 1. Recursive relationship between GetMultiIndex results for different (d, p).

where p_i is a non-negative integer. The main point of the above algorithm is to find all sequences $(p_1, p_2, \cdots, p_d)$ that satisfy the above inequality.

One possible way to implement the algorithm is to automatically generate all possible p^d sequences satisfying $0 \leq p_i \leq p$ $(i = 1, \cdots, d)$ in the first step, and then to remove those sequences for which $p_1 + p_2 + \cdots + p_d > p$ according to the inequality constraints in the second step. However, the first step of this approach leads directly to the curse of dimensionality, which is practically infeasible in the high-dimensional, high-order case.

For this reason, we use a recursive approach to implement this algorithm, denoted by GetMultiIndex(d, p). Fig. 1 demonstrates the recursive relationship between the results of GetMultiIndex for different (d, p).

From Fig. 1, we can easily derive

$$\text{GetMultiIndex}(3,4) = \bigcup_{i=0}^{p} (\text{GetMultiIndex}(d-1, p-i), i).$$

By induction, a general relationship can be obtained as follows

$$\text{GetMultiIndex}(d,p) = \bigcup_{i=0}^{p} (\text{GetMultiIndex}(d-1, p-i), i).$$

Denoting all sequences $(p_1, p_2, \cdots, p_d)$ corresponding to basis functions as multiIndex, and summarizing the above, we obtain Algorithm 1 as follows.

Algorithm 1 Summary of the generation of multiIndex.

Function multiIndex = GetMultiIndex(d, p).
if p == 0
  multiIndex = (0, 0, …, 0); return;
end
if d == 1
  multiIndex = (0, 1, …, p); return;
end
for i = 0: p
  multiIndex =multiIndex ∪ (GetMultiIndex(d-1, p-i), i);
end
end function

This work is licensed under a Creative Commons Attribution-NonCommercial-NoDerivatives 4.0 License. For more information, see https://creativecommons.org/licenses/by-nc-nd/4

This article has been accepted for publication in IEEE Access. This is the author's version which has not been fully edited and content may change prior to final publication. Citation information: DOI 10.1109/ACCESS.2023.3348132

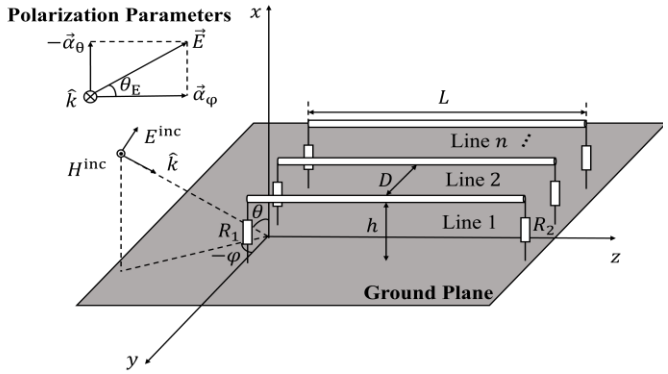

FIGURE 2. **N-conductor TL model under consideration.**

III. APPLICATION OF THE LSPCR METHOD TO MEDIUM AND HIGH DIMENSIONAL TL PROBLEMS

A. PROBLEM STATEMENT

In this paper, a stochastic analysis of a lossless n-conductor (n=10) TL system on an ideal ground, as shown in Fig. 2, is performed using the LSPCR method. The nominal values of its parameters are as follows: the length $L = 10^{-1}$ m, the radius $r = 3 \times 10^{-4}$ m, the height $h = 1.27 \times 10^{-3}$ m, the conductor distance $D = 1.27 \times 10^{-3}$ m, all left terminal load $R_1 = 50\,\Omega$, all right terminal load $R_2 = 100\,\Omega$. This TL system is illuminated by a plane wave with the incidence angle θ, the azimuth angle φ and the polarization angle θ_E, the waveform $E(t) = E_0 e^{-((t-t_0)/T)^2}$, where $E_0 = 1$ kV/m, $t_0 = 1$ ns, $T = 50$ ps. We consider two cases, one for medium random input dimensions and another for high dimensions. Specifically,

Case 1: Assume that the field amplitude E_0, the incidence angle θ, the azimuth angle φ, the polarization angle θ_E, the height h, and the TL radius r (containing 10 parameters) make a total of d = 15 random input parameters, which independently follow the normal distribution with the standard deviation $0.2 * \mu$, where the means of θ and φ, and θ_E are $\mu_\theta = 30^\circ$, and $\mu_\varphi = -45^\circ$, $\mu_{\theta_E} = 45^\circ$, respectively.

Case 2: Assume that the 15 random parameters in case 1 plus the loads at both ends of the TL (which contain 20 parameters) make a total of d =35 random parameters that are mutually independent normal RVs with the standard deviation $0.2 * \mu$, where the mean of the incidence angle θ and the azimuth angle φ, and the polarization angle θ_E are $\mu_\theta = 60^\circ$, and $\mu_\varphi = -30^\circ$, $\mu_{\theta_E} = 60^\circ$, respectively.

In the time domain, the voltage V_i^T and current I_i on the ith conductor follow the following stochastic equation [28], which are

$$\frac{\partial}{\partial z}[V_i^s(z,t,\zeta)] + [L_{ij}(\zeta)]\frac{\partial}{\partial t}[I_i(z,t,\zeta)] = [E_{z_i}^i(z,t,\zeta,h) - E_{z_0}^i(z,t,\zeta,0)], \quad (5a)$$

$$\frac{\partial}{\partial z}[I_i(z,t,\zeta)] + [C_{ij}(\zeta)]\frac{\partial}{\partial t}[V_i^s(z,t,\zeta)] = 0, \quad (5b)$$

$$V_i^T(z,t,\zeta) = V_i^s(z,t,\zeta) + V_i^i(z,t,\zeta), \quad (5c)$$

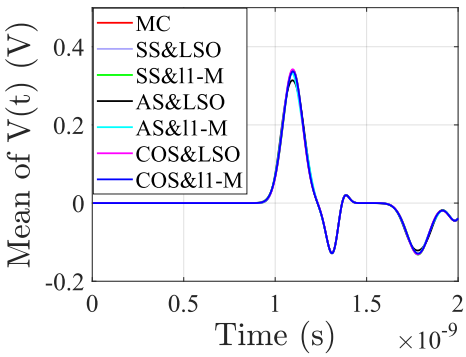

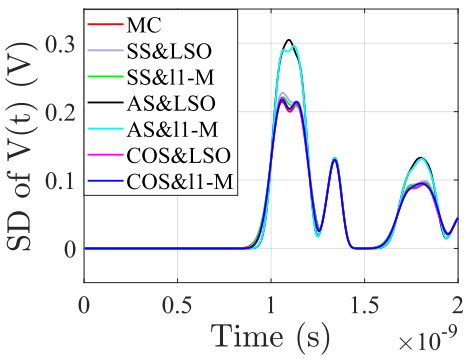

(a)

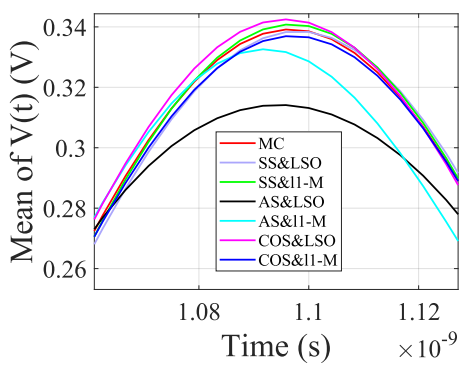

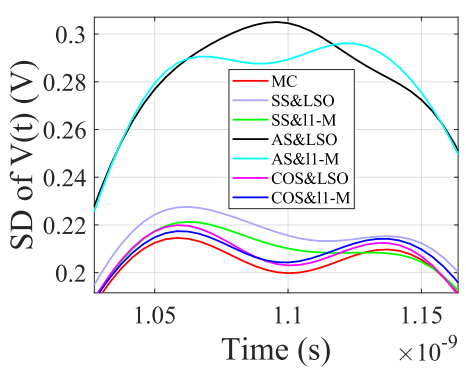

(b)

FIGURE 3. **Plots for, (a) moments of the six LSPCR and MC solutions, and (b) zoom-in results for d = 15.**

where

$$V_i^i(z,t,\zeta) = \int_0^h E_{\eta_i}^i(\eta_i,z,t,\zeta)d\eta_i,$$

This work is licensed under a Creative Commons Attribution-NonCommercial-NoDerivatives 4.0 License. For more information, see https://creativecommons.org/licenses/by-nc-nd/4

This article has been accepted for publication in IEEE Access. This is the author's version which has not been fully edited and
content may change prior to final publication. Citation information: DOI 10.1109/ACCESS.2023.3348132

V_i^s is the scattered (induced) voltage on the ith conductor, $E_{z_i}^i$ is the z-component of the total electric field (line axis) on the ith conductor, $[L_{ij}]$ is the inductance-per-unit-length matrix, $[C_{ij}]$ is the capacitance-per-unit-length matrix of the multi-conductor line, V_i^i is the incident voltage on the ith conductor, ξ is a random vector.

B. NUMERICAL REALIZATION

In the six algorithms for solving stochastic multi-conductor TLs, all numerical experiments were carried out on a workstation with two Intel Xeon Gold 6226R CPUs and 192GB of memory. When implementing the six algorithms, the highest order of the basis functions $p = 2$ is chosen. This implies the number of basis functions $P = 136$ for $d = 15$, $P = 666$ for $d = 35$. A common $\delta = 10^{-4}$ is selected for the ℓ_1-Ms. The Hermite polynomials are chosen as the basis functions because the random parameters all follow a normal distribution. In the numerical experiment, independent replicate experiments were carried out for each sample N and the experimental results were averaged to eliminate the evaluation errors associated with the randomness of the PCE coefficients resulting from the stochastic nature of the samples generated each time.

It is worth noting that once the stochastic problem is given, all the factors that can influence the numerical solution of the LSPCR are: the highest order p which determines the number of the basis functions, the number of samples N, the randomness of the samples that has been essentially eliminated by independent replicate experiments, the choice of sampling strategy and the norm problem, respectively. In fact, the aim of this paper is to explore the differences in accuracy and efficiency of the six different algorithms formed by the combination of three sampling strategies with two types of norm problems in the medium-dimensional, low-order and high-dimensional, low-order cases.

1) IMPLEMENTATION OF THE SIX LSPCR ALGORITHMS

The six algorithms are designed to calculate the coefficients in (2), and generate the first two moments of random voltage responses from these coefficients. Fig. 3 shows the time-domain voltage response moments at the right-terminal termination point of the sixth TL for $d = 15$ random parameters derived between the reference and six algorithms, using the moments of the MC solution for $N = 10^5$ samples as the reference. This is because when N is greater than 10^5, the MC moments hardly show changes, but any decrease in N causes changes. Fig. 4 shows the counterparts for $d = 35$. Similarly, for $d = 35$, the moments of the MC solution for $N = 2 \times 10^5$ samples are chosen to serve as the reference. For the six algorithms, we take $N = 300$ samples for $d = 15$, and $N = 1400$ samples for $d = 35$.

It can be seen from Figs. 3 and 4 that the moments of the SSs, the COSs agree very well with the reference, while the means of the ASs agree better with the reference, but with a greater difference in the standard deviation (SD).

It is worth noting that in the low-order, low-dimensional case, as with the other four algorithms, the ASs also obtain high accuracy in the solution moments [26]. A similar situation can be seen in Fig. 5, which is obtained by solving the model in Fig. 2 with $d = 3$ random input parameters, where the incidence angle θ, the azimuth angle φ and the

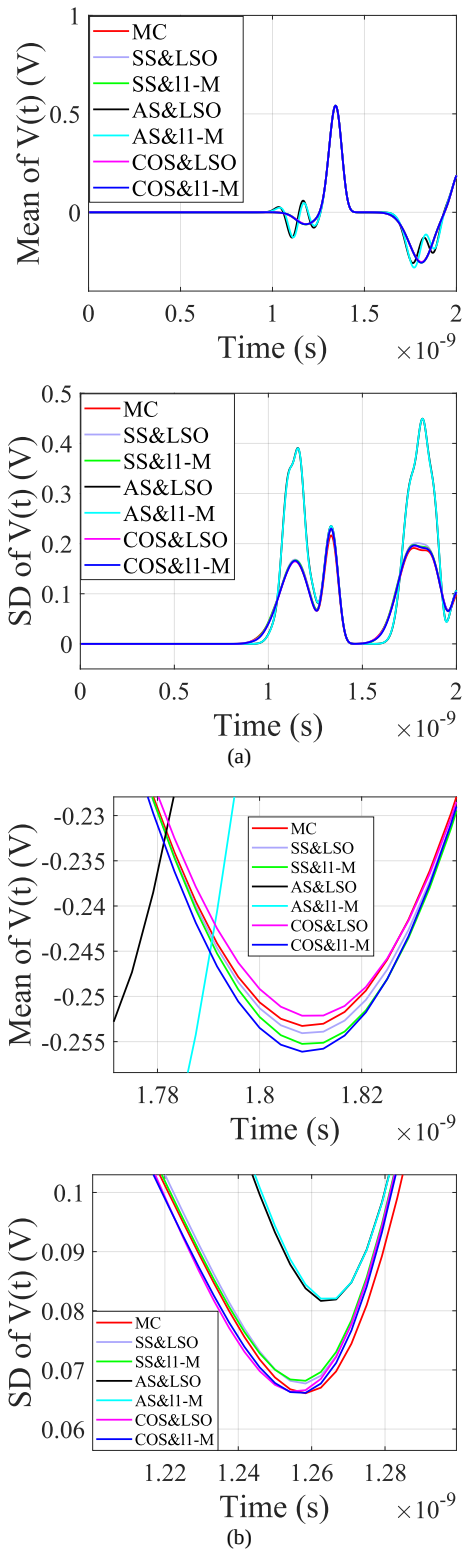

FIGURE 4. Plots for, (a) moments of the six LSPCR and MC solutions, and (b) zoom-in results for $d = 35$.

This work is licensed under a Creative Commons Attribution-NonCommercial-NoDerivatives 4.0 License. For more information, see https://creativecommons.org/licenses/by-nc-nd/4

This article has been accepted for publication in IEEE Access. This is the author's version which has not been fully edited and
content may change prior to final publication. Citation information: DOI 10.1109/ACCESS.2023.3348132

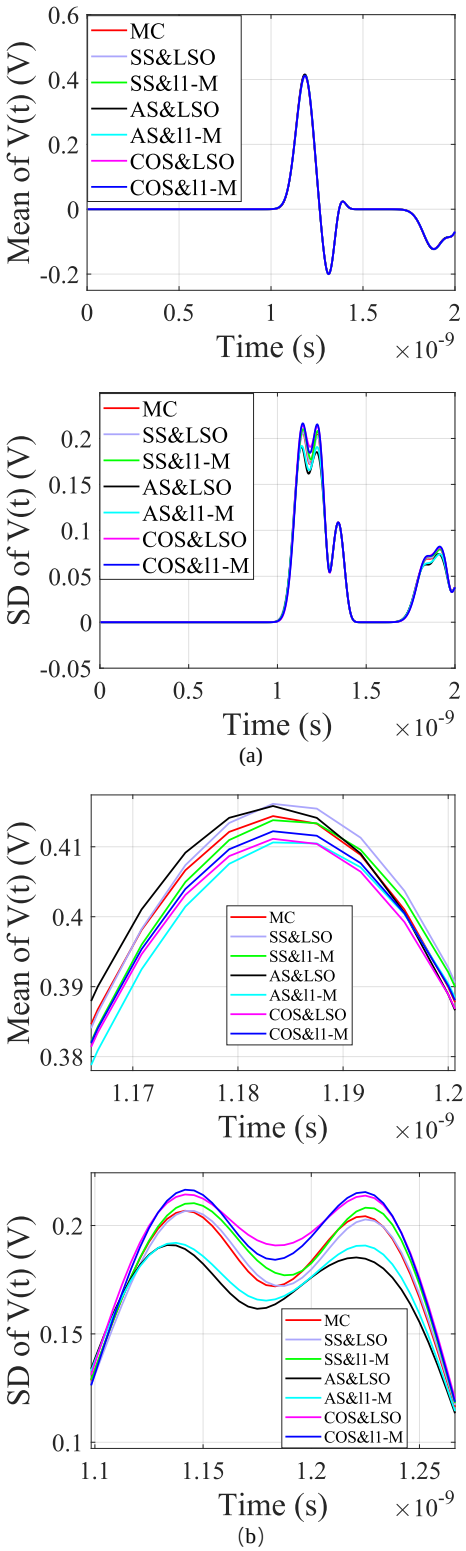

FIGURE 5. **Plots for, (a) moments of the six LSPCR and MC solutions, and (b) zoom-in results for $d = 3$.**

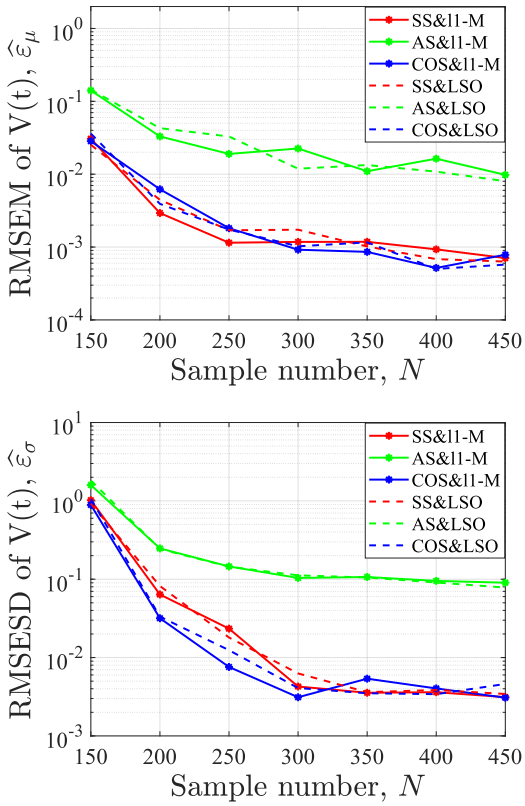

FIGURE 6. **Computed $\hat{\varepsilon}$ of the moments derived between the reference and six algorithms with $d = 15$ as a function of N.**

TABLE I
COMPUTING COST COMPARISON FOR THE SIX ALGORITHMS WITH D=15

Time (s)	SS	AS	COS
LSO	3511	3582	3701
ℓ_1-M	3674	3691	3955

polarization angle θ_E vary randomly.

It can be seen from [26] and Fig. 5 that the AS performs almost as excellently as the COS in the low-dimensional case, while Figs. 3 and 4 show that it performs poorly in the high-dimensional case. If attempting to increase p to achieve a high accuracy solution in this case, it would suffer from the extremely enormous curse of dimensionality. Therefore, the AS is better suited to solving low-dimensional problems.

2) COMPARISON OF SIX ALGORITHMS WITH DIFFERENT NUMBER OF SAMPLES

In order to more accurately and easily compare the differences between the six algorithms for different N, we define relative mean square error of the mean (RMSEM) $\hat{\varepsilon}_\mu$ and relative mean square error of the standard deviation (RMSESD) $\hat{\varepsilon}_\sigma$ to describe the accuracy of the mean and the standard deviation,

$$\hat{\varepsilon}_\mu := \frac{\int_T E\big(\mu(t) - \mu_{\mathrm{Ref}}(t)\big)^2 \mathrm{d}t}{\int_T E(\mu^2_{\mathrm{Ref}}(t))\mathrm{d}t}, \tag{6a}$$

$$\hat{\varepsilon}_\sigma := \frac{\int_T E(\sigma(t) - \sigma_{\mathrm{Ref}}(t))^2 \mathrm{d}t}{\int_T E(\sigma^2_{\mathrm{Ref}}(t))\mathrm{d}t}, \tag{6b}$$

This work is licensed under a Creative Commons Attribution-NonCommercial-NoDerivatives 4.0 License. For more information, see https://creativecommons.org/licenses/by-nc-nd/4

This article has been accepted for publication in IEEE Access. This is the author's version which has not been fully edited and
content may change prior to final publication. Citation information: DOI 10.1109/ACCESS.2023.3348132

where T is the observation time, E denotes the expectation operator, $\mu(t)$ and $\sigma(t)$ are the mean and the standard deviation derived from the LSPCR method, $\mu_{\mathrm{Ref}}(t)$ and $\sigma_{\mathrm{Ref}}(t)$ are the reference. We still choose the moments of the MC solution in section 1) as the reference.

Fig. 6 plots the computed $\hat{\varepsilon}$ of the moments derived between the reference and six algorithms with $d = 15$ as a function of N, and Fig. 7 shows the counterparts for $d = 35$.

It can be seen from Figs. 6 and 7 that the moment accuracies gradually increase as N increases because the computed $\hat{\varepsilon}$ values corresponding to the six algorithms gradually decrease. Furthermore, we find that when $N/P \geq 2.1$ (i.e., $N \geq 300$ for $d = 15$, $N \geq 1400$ for $d = 35$), both the SSs and the COSs recover moments with high accuracy because their $\hat{\varepsilon}$ values are very small, while the ASs recover moments with low accuracy because their $\hat{\varepsilon}$ values are large. In addition, there are no noticeable differences between the ℓ_1-Ms and the LSOs, as well as between the SSs and the COSs, since their $\hat{\varepsilon}$ values are not significantly different.

To compare the efficiency, N=300 samples for $d = 15$ and N=1400 samples for $d = 35$ are taken. The average computation time is shown in TABLE I and II.

Note that the computation time for the reference is 616493 s for d = 15 and 1243669 s for d = 35. Compared to TABLE I and II, this implies that the LSPCR method requires no more than 0.7% of the MC calculation time for d=15, and no more than 1.4% of the MC calculation time for d=35. Compared to the reference, the SSs and the COSs show a great improvement in efficiency with similar accuracy of the moments. Furthermore, TABLE I and II also show that the LSOs have a significant speed advantage over the ℓ_1-Ms. In addition, the SSs and the ASs are obviously faster than the COSs, and there are small differences between the SSs and the ASs.

IV. CONCLUSION

This paper proposes an algorithm based on the recursive idea to solve the problem of automatically determining the basis function composed of a large number of multivariate polynomials, which is usually faced in the implementation of PCE programs in the high-dimensional case, and combines this algorithm with the latest weight-based regression called LSPCR, and then proposes the implementation of the LSPCR method in the medium- and high-dimensional cases, and evaluates its performance in the electromagnetic coupling problem of the TL in this case. Six algorithms for LSPCR have been designed and implemented and are then compared with the MC method and with each other.

Numerical experiments demonstrate the excellence of the proposed algorithm. Furthermore, the results also show that for the medium- or high-dimensional, low-order problems, compared to the MC, only the SSs, and the COSs show a great improvement in efficiency with similar accuracy of the moments. Moreover, the SSs and the COSs outperform the ASs, and there is almost no difference between the ℓ_1-Ms and the LSOs, as well as between the SSs and the COSs. In addition, the ℓ_1-Ms are obviously slower than the LSOs. The SSs and the ASs are obviously faster than the COSs, and there are small differences between the SSs and the ASs.

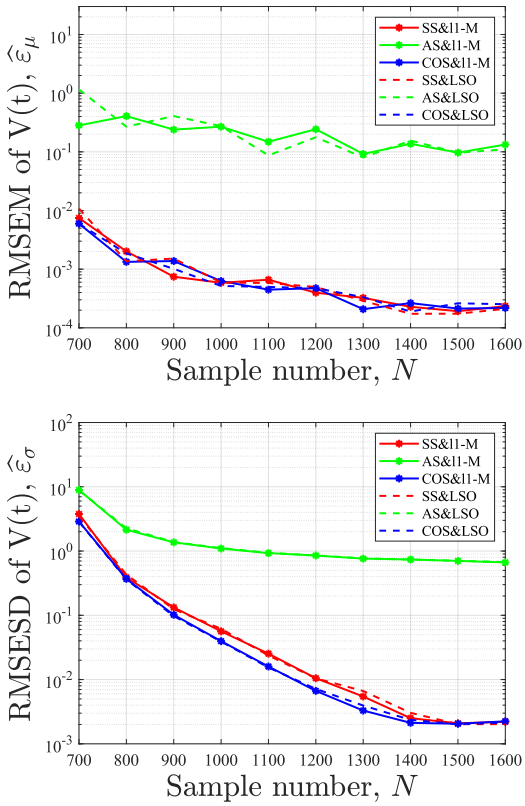

FIGURE 7. Computed $\hat{\varepsilon}$ of the moments derived between the reference and six algorithms with $d = 35$ as a function of N.

TABLE II
COMPUTING COST COMPARISON FOR THE SIX ALGORITHMS WITH D=35

Time (s)	SS	AS	COS
LSO	13916	13808	17321
ℓ_1-M	14656	14580	17663

REFERENCES

[1] T. E. Lovett, F. Ponci and A. Monti, "A polynomial chaos approach to measurement uncertainty," *IEEE Transactions on Instrumentation and Measurement*, vol. 55, no. 3, pp. 729-736, June 2006.

[2] G. D'Antona, A. Monti, F. Ponci and L. Rocca, "Maximum Entropy Multivariate Analysis of Uncertain Dynamical Systems Based on the Wiener–Askey Polynomial Chaos," *IEEE Transactions on Instrumentation and Measurement*, vol. 56, no. 3, pp. 689-695, June 2007.

[3] P. Voglewede, A. H. C. Smith and A. Monti, "Dynamic Performance of a SCARA Robot Manipulator With Uncertainty Using Polynomial Chaos Theory," *IEEE Transactions on Robotics*, vol. 25, no. 1, pp. 206-210, Feb. 2009.

[4] H. Acikgoz and R. Mittra, "Stochastic Polynomial Chaos Expansion Analysis of a Split-Ring Resonator at Terahertz Frequencies," *IEEE Transactions on Antennas and Propagation*, vol. 66, no. 4, pp. 2131-2134, April 2018.

[5] I. S. Stievano, P. Manfredi and F. G. Canavero, "Parameters Variability Effects on Multiconductor Interconnects via Hermite Polynomial Chaos," *IEEE Transactions on Components, Packaging and Manufacturing Technology*, vol. 1, no. 8, pp. 1234-1239, Aug. 2011.

This work is licensed under a Creative Commons Attribution-NonCommercial-NoDerivatives 4.0 License. For more information, see https://creativecommons.org/licenses/by-nc-nd/4

This article has been accepted for publication in IEEE Access. This is the author's version which has not been fully edited and
content may change prior to final publication. Citation information: DOI 10.1109/ACCESS.2023.3348132

[6] Q. Su and K. Strunz, "Stochastic Polynomial-Chaos-Based Average Modeling of Power Electronic Systems," *IEEE Transactions on Power Electronics*, vol. 26, no. 4, pp. 1167-1171, April 2011.
[7] S. L. Ho and S. Yang, "A Fast Robust Optimization Methodology Based on Polynomial Chaos and Evolutionary Algorithm for Inverse Problems," *IEEE Transactions on Magnetics*, vol. 48, no. 2, pp. 259-262, Feb. 2012.
[8] A. C. M. Austin and C. D. Sarris, "Efficient Analysis of Geometrical Uncertainty in the FDTD Method Using Polynomial Chaos With Application to Microwave Circuits," *IEEE Transactions on Microwave Theory and Techniques*, vol. 61, no. 12, pp. 4293-4301, Dec. 2013.
[9] P. Manfredi, D. Vande Ginste, D. De Zutter and F. G. Canavero, "On the Passivity of Polynomial Chaos-Based Augmented Models for Stochastic Circuits," *IEEE Transactions on Circuits and Systems I: Regular Papers*, vol. 60, no. 11, pp. 2998-3007, Nov. 2013.
[10] M. R. Rufuie, E. Gad, M. Nakhla and R. Achar, "Generalized Hermite Polynomial Chaos for Variability Analysis of Macromodels Embedded in Nonlinear Circuits," *IEEE Transactions on Components, Packaging and Manufacturing Technology*, vol. 4, no. 4, pp. 673-684, April 2014.
[11] M. R. Rufuie, E. Gad, M. S. Nakhla and R. Achar, "Fast Variability Analysis of General Nonlinear Circuits Using Decoupled Polynomial Chaos," *IEEE Transactions on Components, Packaging and Manufacturing Technology*, vol. 5, no. 12, pp. 1860-1871, Dec. 2015.
[12] Y. Xu, L. Mili, A. Sandu, M. R. v. Spakovsky and J. Zhao, "Propagating Uncertainty in Power System Dynamic Simulations Using Polynomial Chaos," *IEEE Transactions on Power Systems*, vol. 34, no. 1, pp. 338-348, Jan. 2019.
[13] C. Qiu, X. Peng, Z. Liu and J. Tan, "Sensitivity Analysis of Random and Interval Uncertain Variables Based on Polynomial Chaos Expansion Method," *IEEE Access*, vol. 7, pp. 73046-73056, 2019.
[14] G. J. K. Tomy and K. J. Vinoy, "A Fast Polynomial Chaos Expansion for Uncertainty Quantification in Stochastic Electromagnetic Problems," *IEEE Antennas and Wireless Propagation Letters*, vol. 18, no. 10, pp. 2120-2124, Oct. 2019.
[15] X. Wang, X. Wang, H. Sheng and X. Lin, "A Data-Driven Sparse Polynomial Chaos Expansion Method to Assess Probabilistic Total Transfer Capability for Power Systems With Renewables," *IEEE Transactions on Power Systems*, vol. 36, no. 3, pp. 2573-2583, May 2021.
[16] Q. Wang, Y. Zhao and Q. Wu, "Stochastic Quantification of Array Antennas With Random Feeding Errors Using an Improved Polynomial Chaos Expansion Method," *IEEE Antennas and Wireless Propagation Letters*, vol. 21, no. 12, pp. 2347-2351, Dec. 2022.
[17] Y. Wan, D. E. Shen, S. Lucia, R. Findeisen and R. D. Braatz, "A Polynomial Chaos Approach to Robust Static Output-Feedback Control With Bounded Truncation Error," *IEEE Transactions on Automatic Control*, vol. 68, no. 1, pp. 470-477, Jan. 2023.
[18] H. Rogier, "Generalized Gamma-Laguerre Polynomial Chaos to Model Random Bending of Wearable Antennas," *IEEE Antennas and Wireless Propagation Letters*, vol. 21, no. 6, pp. 1243-1247, June 2022.
[19] Z. Zhang, T.W. Weng, and L. Daniel, "Big-data tensor recovery for high-dimensional uncertainty quantification of process variations," *IEEE Trans. Compon., Packag., Manuf. Technol.*, vol. 7, no. 5, pp. 687–697, May 2017.
[20] P. Manfredi, "A hierarchical approach to dimensionality reduction and nonparametric problems in the polynomial chaos simulation of TL," *IEEE Trans. Electromagn. Compat.*, vol. 62, no. 3, pp. 736-745, Jun. 2020.
[21] X. Wu, P. Manfredi, D. Vande Ginste, and F. Grassi, "A hybrid perturbative stochastic Galerkin method for the variability analysis of nonuniform TL," *IEEE Trans. Electromagn. Compat.*, vol. 62, no. 3, pp. 746-754, Jun. 2020.
[22] M. Yusuf and S. Roy, "A polymorphic polynomial chaos formulation for mixed epistemic-aleatory uncertainty quantification of RF/microwave circuits," *IEEE Trans. Microw. Theory Techn.*, vol. 70, no. 1, pp. 926–937, Jan. 2022.
[23] J. Laowanitwattana and S. Uatrongjit, "Probabilistic Power Flow Analysis Based on Partial Least Square and Arbitrary Polynomial Chaos Expansion," *IEEE Trans. Power Systems*, vol. 37, no. 2, pp. 1461-1470, March 2022.
[24] J. Hampton and A. Doostan, "Coherence motivated sampling and convergence analysis of least squares polynomial chaos regression," *Comput Methods Appl. Mech. Eng.*, 290:73–97, 2015.
[25] J. Hampton and A. Doostan, "Compressive sampling of polynomial chaos expansions: convergence analysis and sampling methods," *J. Comput. Phys.*, 280, pp. 363–386, 2015.
[26] W. Chen, S. H. Zhou, R. Fan, Y. Zhang, L. Yan and X. Zhao, "Least squares polynomial chaos regression for stochastic analysis of transmission lines without and with noise," *IEEE Transactions on Components, Packaging and Manufacturing Technology*, vol. 13, no. 5, pp. 675-687, May 2023.
[27] D. Xiu and G. Karniadakis, "The Wiener–Askey polynomial chaos for stochastic differential equations," *SIAM J. Sci. Comput.*, 24 (2), pp. 619–644, 2002.
[28] A. K. Agrawal, H. J. Price, and S. H. Gurbaxani, "Transient response of multiconductor transmission lines excited by a nonuniform electromagnetic field," *IEEE Trans. Electromagn. Compat.*, vol. 22, no. 2, pp. 119– 129, May 1980.

Weiwei Chen received the M.S. degree in fundamental mathematics from Sichuan University, Chengdu, China, in 2018. He is currently working towards the Ph.D. degree in information and communication engineering at Sichuan University.

His research interests include uncertainty quantification, computational electromagnetics, electromagnetic compatibility, differential equations and dynamical systems.

Yuhang Ji received the B.S. degree in Electronic Information Science and Technology from Sichuan University, Chengdu, China, in 2022. He is currently working towards the Ph.D. degree in Information and Communication Engineering at Sichuan University.

His research interests include computational electromagnetics, electromagnetic compatibility modelling.

Ziyang Qi received the B.S. degree in electronic information engineering from Sichuan University, Chengdu, China, in 2021. he is currently pursuing the M.S. degree in electronic information from Sichuan University, Chengdu, China.

His research interests include electromagnetic compatibility modelling and computational electromagnetics.

Liping Yan (M'08-SM'15) received the M.S. degree in radio physics and the Ph.D. degree in biomedical engineering from Sichuan University, Chengdu, China, in 1996 and 2003, respectively.

In 1996, she joined the department of electronics engineering at Sichuan University. From Mar. 2008 to Mar. 2009. she was a visiting scholar of the Department of Electrical Engineering and Computer Science at the University of Wisconsin in Milwaukee. Since July 2009, she has been working as a professor with the college of Electronics and Information Engineering, Sichuan University, Chengdu, China. She has authored/co-authored 1 book, more than 100 papers published in peer-reviewed journals and international conferences and led a number of industrial/grant projects. Her research interests include electromagnetic environment effects, electromagnetic compatibility modeling, computational electromagnetics,

This work is licensed under a Creative Commons Attribution-NonCommercial-NoDerivatives 4.0 License. For more information, see https://creativecommons.org/licenses/by-nc-nd/4

This article has been accepted for publication in IEEE Access. This is the author's version which has not been fully edited and
content may change prior to final publication. Citation information: DOI 10.1109/ACCESS.2023.3348132

design of applicators/probes for biomedical applications, and compact antennas.

Xiang Zhao received the M.S. degree in radio physics and the Ph.D. degree in biomedical engineering from the Sichuan University, Chengdu, China, in 1997 and 2005, respectively.

In 1997, she joined the department of electronics engineering. Since 2012, she has been a professor with the College of Electronics and Information Engineering, Sichuan University, Chengdu, China. She has published over 90 papers in the peer-reviewed journals and conferences and led a number of grant projects. Her research interests include statistical electromagnetics, electromagnetic compatibility modeling and electromagnetic environment effects evaluation.

This work is licensed under a Creative Commons Attribution-NonCommercial-NoDerivatives 4.0 License. For more information, see https://creativecommons.org/licenses/by-nc-nd/4